Published in final edited form as:

BJU Int. 2018 February ; 121(2): 301–312. doi:10.1111/bju.13985.

Controlled release of insulin-like growth factor 1 enhances urethral sphincter function and histological structure in the treatment of female stress urinary incontinence in a rat model

Hao Yan[#*,†], **Liren Zhong**[#‡,§], **Yaodong Jiang**[#‡,§], **Jian Yang**[‡], **Junhong Deng**[¶], **Shicheng Wei**[**], **Emmanuel Opara**[§], **Anthony Atala**[‡], **Xiangming Mao**[††], **Margot S. Damaser**[*,‡‡,§§], **Yuanyuan Zhang**[‡]

[*]Biomedical Engineering Department of the Lerner Research Institute, Cleveland, OH, USA

[†]Department of Urology, Xuanwu Hospital, Capital Medical University, Beijing, China

[‡]Institute for Regenerative Medicine, Wake Forest University, Winston-Salem, NC, USA

[§]Department of Urology, Nanfang Hospital, Southern Medical University, Guangzhou, China

[¶]Department of Andrology, The First People's Hospital of Guangzhou, Guangzhou, Guangdong, China

[**]Laboratory of Biomaterials and Regenerative Medicine, Academy for Advanced Interdisciplinary Studies, Peking University, Beijing, China

[††]Department of Urology, Zhujiang Hospital, Southern Medical University, Guangzhou, China

[‡‡]The Advanced Platform Technology Center of the Louis Stokes Cleveland VA Medical Center, Cleveland, OH, USA

[§]Glickman Urological and Kidney Institute, Cleveland Clinic, Cleveland, OH, USA

[#] These authors contributed equally to this work.

Abstract

Objectives—To determine the effects of controlled release of insulin-like growth factor 1 (IGF-1) from alginate-poly-L-ornithine-gelatine (A-PLO-G) microbeads on external urethral sphincter (EUS) tissue regeneration in a rat model of stress urinary incontinence (SUI), as SUI diminishes the quality of life of millions, particularly women who have delivered vaginally, which can injure the urethral sphincter. Despite several well-established treatments for SUI, growth factor therapy might provide an alternative to promote urethral sphincter repair.

Materials and Methods—In all, 44 female Sprague-Dawley rats were randomised into four groups: vaginal distension (VD) followed by periurethral injection of IGF-1-A-PLO-G microbeads

Correspondence: Wake Forest Institute For Regenerative Medicine, 391 Technology way, Winston-Salem, NA 27101, USA. yzhang@wakehealth.edu and Xiangming Mao, Department of Urology, Nanfang Hospital, Southern Medical University, Guangzhou, Guangdong, China. 13802503635@126.com.

Conflicts of Interest

None.

(VD + IGF-1 microbeads; 1×10^4 microbeads/1 mL normal saline); VD + empty microbeads; VD + saline; or sham-VD + saline (sham).

Results—Urethral function (leak-point pressure, LPP) was significantly lesser 1 week after VD + saline [mean (SEM) 23.9 (1.3) cmH_2O] or VD + empty microbeads [mean (SEM) 21.7 (0.8) cmH_2O) compared to the sham group [mean (SEM) 44.4 (3.4) cmH_2O; $P < 0.05$), indicating that the microbeads themselves do not create a bulking or obstructive effect in the urethra. The LPP was significantly higher 1 week after VD + IGF-1 microbeads [mean (SEM) 28.4 (1.2) cmH_2O] compared to VD + empty microbeads ($P < 0.05$), and was not significantly different from the LPP in sham rats, demonstrating an initiation of a reparative effect even at 1 week after VD. Histological analysis showed well-organised skeletal muscle fibres and vascular development in the EUS at 1 week after VD + IGF-1 microbeads, compared to substantial muscle fibre attenuation and disorganisation, and less vascular formation at 1 week after VD + saline or VD + empty microbeads.

Conclusion—Periurethral administration of IGF-1-A-PLO-G microbeads facilitates recovery from SUI by promoting skeletal myogenesis and revascularisation. This therapy is promising, but detailed and longer term studies in animal models and humans are needed.

Keywords

external urethral sphincter; vascularisation; microbeads; rat; female

Introduction

Several minimally invasive surgical therapies, including sling surgical procedures [1] and injection of bulking agents [2–9] are used to treat stress urinary incontinence (SUI) [10]. Although the sling procedure can reinforce weak pelvic floor muscles and has reported success rates of 71–73% [1], the urethral sphincter deficiency remains [11]. Injection of bulking agents has provided encouraging outcomes, but over time these agents are absorbed and can cause chronic inflammation, periurethral abscesses, foreign body giant cell responses, erosion of the urinary bladder or the urethra, migration to inner organs, obstruction of the lower urinary tract with resultant urinary retention and severe voiding dysfunction, and even pulmonary embolism [9,12,13].

Growth factor therapy involves the use of growth factors to promote endogenous tissue regeneration or wound healing [14], either alone or with cell therapy. Growth factors released from biodegradable microbeads or gels can be locally applied to improve cell survival, differentiation, and life-span of the grafted cells when injected with stem cells [15], and stimulation of endogenous stem cells to participate into tissue injury repair and closure [16]. Growth factor therapy could provide a potential ‘off-the-shelf’ product for use clinically.

Insulin-like growth factor 1 is an important mediator in multiple developmental processes, such as cell proliferation, anti-apoptosis, myogenic differentiation, innervation, and angiogenesis [17]. IGF-1 plays an important role in childhood growth and continues to have anabolic effects in adults. As a therapeutic agent, it is used in the treatment of patients with

severe primary IGF-1 deficiency or Laron syndrome [18]. Several studies using animal models of urinary sphincter dysfunction have shown that systemic or local administration of IGF-1 promotes physiological skeletal growth, reduces apoptosis and collagen deposition, enhances angiogenesis, and restores innervation, ultimately leading to recovery from SUI [19]. However, the disadvantages of systemic IGF-1 administration include limited effect due to the short half-life of IGF-1, as well as potential cancer-related toxicity, vasodilation, tachycardia, and hypoglycaemia [20]. Therefore, controlled locally sustained delivery of IGF-1 should result in safer and more effective sphincter tissue repair.

In the present study, we used a novel controlled-drug-release system, alginate-poly-L-ornithine-gelatine (A-PLO-G) microbeads compared to traditional A-PLO microbeads [21], to determine the efficacy of IGF-1 released from A-PLO-G microbeads in the restoration of the injured external urethral sphincter (EUS) in a rat model of SUI created via vaginal distention (VD), with the goal of developing an improved therapy for SUI.

Materials and Methods

Study Design

This study was approved by the Institute of Animal Use and Care Committees of both Cleveland Clinic and the Institute for Regenerative Medicine of Wake Forest University. In all, 44 nulliparous female adult Sprague-Dawley rats (200–225 g) were randomly allocated into four groups and underwent VD treated with IGF-1 loaded A-PLO-G microbeads (VD + IGF-1 microbeads); VD treated with empty A-PLO-G microbeads (VD + empty microbeads); VD treated with normal saline (VD + saline); or sham-VD treated with saline (Sham). At 1 week after VD or sham-VD all the rats underwent leak-point pressure (LPP) assessment with EUS electromyography (EMG) testing and the urethra was then harvested for histological and immunohistochemical assessment.

Preparation of A-PLO and A-PLO-G Microbeads

Chemicals—Chemicals and reagents used in this study included: sodium chloride (NaCl), calcium chloride ($CaCl_2$), EDTA, mineral oil, Span80® (Sigma-Aldrich, St. Louis, MO, USA), acetic acid, gelatine, PLO hydrochloride ($1.5–3 \times 10^4$ molecular weight; Sigma-Aldrich), human IGF-1 (Abcam, Cambridge, MA, USA), and Hanks' Balanced Salt Solution (HBSS; Thermo Fisher Scientific, Waltham, MA, USA). In addition, we used low viscosity (20–200 mPa/s) ultra-pure sodium alginates with high mannuronic acid content, i.e. low viscosity monomer (LVM; Nova-Matrix, Oslo, Norway), molecular weights of 75–200 kDa and a guluronic/mannuronic ratio of ≤1 and ≥1.5, respectively.

Solutions—Alginate solution (3%) and EDTA-Ca (100 mM) are mixed in a volume ratio of 1:1 to prepare the alginate-EDTA-Ca solution (1.5% LVM), and then stored at 4 °C until required. Span mineral oil (2%) was prepared with 0.2 mL Span80 and 9.8 mL mineral oil. A 0.5% glacial acetic acid mineral oil was made from 50 μL glacial acetic acid and 10 mL mineral oil. IGF-1 was reconstituted with 5 mmol/L sodium phosphate to a final concentration of 1 mg/mL.

Generation of A-PLO and A-PLO-G Microbeads—Microcapsules were prepared in a biosafety cell culture hood under sterile conditions. LVM (1.5%) was extruded through an eight-channel microfluidic device at a flow rate of 1 μL/min to form 100-μm diameter capsules, which were extruded into a 100 mmol/L $CaCl_2$ solution, and allowed to crosslink for 5 min. Microbeads were then transferred to an Eppendorf tube and rinsed twice with a mixture of 22 mmol/L $CaCl_2$ and 0.9% NaCl, and once with 1% v/v Tween 20 solution. Microbeads were then mixed with either 10 μL ultrapure water (empty microbeads as a control) or 10 μL of 1 mg/mL IGF-1 and shaken at 4 °C overnight. The microbeads were subsequently placed in a 0.3% PLO solution and rocked to form A-PLO-IGF-1 microbeads [21] for 1 h. To generate A-PLO-G-IGF-1 microbeads, A-PLO-IGF-1 beads were mixed with 0.245% gelatine solution and rocked for 10 min. Finally, the microbeads were rinsed with a mixture of 22 mmol/L $CaCl_2$ and 0.9% NaCl to remove the unbound gelatine and prepare for injection. Both IGF-1-encapsulated microbeads and empty microbeads were tested for integrity and homogeneity of the microbeads after injection into a culture dish via a 26-G syringe needle (nominal inner diameter 260 μm) and then prepared in advance and stored at 4 °C until used.

Testing the Retention of Microbeads *In Vivo*

To evaluate the retention of microbeads around urethral tissue after periurethral injection, A-PLO (five rats) was injected into female adult Sprague-Dawley rats after being anaesthetised with 2% isoflurane and compared to the injection of A-PLO-G microbeads as a control (five rats). A 10-mm segment of the mid-urethra, attached to the anterior portion of the vagina (10-mm proximal to the urethral meatus), was dissected, immersion fixed in 10% formalin and sectioned transversely (5 μm) for histological analysis (see below). A-PLO-G microbeads were found around the urethral tissue, but no A-PLO microbeads were detected. Therefore, IGF-1 release assessment and the functional and anatomical experiments were done only with A-PLO-G microbeads.

Measurement of IGF-1 Release

Insulin-like growth factor 1 loaded A-PLO-G microbeads were placed in a 22 mmol/L $CaCl_2$ solution (pH 7.2) and incubated on a rotating incubator at 37 °C. The buffer was replaced at 10 time points, i.e. 1, 6, 12, 24 and 36 h; and then at 2, 3, 4, 5, 8 and 14 days. The amount of IGF-1 released into the PBS was assessed by ELISA, performed according to the manufacturer's instructions (Quantikine Human FGF Basic Immunoassay; R&D Systems, Minneapolis, MN, USA).

Establishment of the SUI Rat Model

After successful induction of anaesthesia with 2% isoflurane, the vagina was accommodated with increasing sizes of lubricated Otis bougie à boule urethral dilators (24–32 F) to avoid rupturing the vagina, as described previously [22]. For VD, a modified 10-F Foley balloon catheter was then inserted into the vagina. Although a balloon filled with 5 mL has been used previously by some investigators to create VD and SUI in rats [23], we filled the Foley balloon to 3 mL to create VD and SUI as we have done previously [22,24–27]; as in the small rats (200–225 g) used in this study, filling the balloon to 5 mL results in high

mortality. The Foley balloon was slowly inflated with water to 3 mL and a suture was placed in the perineum to keep the balloon in place for 4 h, after which time the balloon was deflated, the suture was removed, and the catheter was withdrawn from the vagina. Sham-VD consisted of all procedures for VD without inflation of the balloon.

Whilst the rats were still under anaesthesia, 1×10^4 microbeads in 1 mL normal saline were injected periurethrally through a 26-G needle in two injections down the length of the urethra at approximately the 5 and 7 O'clock positions, starting the injection at the bladder neck and injecting while withdrawing the needle. Rats in the VD + saline and sham groups received similar injections but with only saline. Rats were given bupenorphrine (0.1 mg/kg, s.c., twice daily for 3 days) for pain control.

Urethral Function Testing

At 1 week after VD or sham-VD, rats were anaesthetised with isoflurane and a polyethylene catheter (PE-50) was inserted suprapubically into the bladder dome and fixed with a 6-0 silk purse-string suture. The abdominal wall was then sutured closed and the catheter was connected to a pressure transducer (Model P300; Grass Instruments, West Warwick, RI, USA) and a syringe pump (Model 200; KD Scientific, New Hope, PA, USA) to both measure bladder pressure and fill the bladder (5 mL/h). After carefully exposing the urethra by opening the pubic symphysis with forceps, isoflurane anaesthesia was removed and replaced with urethane anaesthesia (1.2 g/kg, intraperitoneal), as urethane best preserves the reflexes of the lower urinary tract [28]. A parallel platinum bipolar electrode (tip diameter 125 mm, PBSA1075; FHC, Bowdoin, ME, USA), connected to a recording system (model P511; AC Amplifier, Astro-Med Inc., West Warwick, RI, USA), was then placed at the midurethra to record EUS EMG, as we have done previously [25].

To determine LPP, with the bladder approximately half full, intravesical pressure was gradually increased by slowly and gently pressing directly on the bladder with a cotton-tipped applicator, whilst both bladder pressure and EUS EMG were amplified (Model P122; Grass Instruments), filtered (60 and 120 Hz), and recorded with an analogue-to-digital recording system (10-kHz sampling rate; band-pass frequencies: 3 Hz–3 kHz; Power-Lab 8/35; AD Instruments, Colorado Springs, CO, USA). LPP was calculated by subtracting baseline pressure from peak bladder pressure at the moment of leakage during LPP testing [29]. One second segments of EUS EMG data were selected at baseline pressure just before LPP testing and at the point of peak pressure during LPP testing. Using a 15-mV threshold, mean EMG amplitude and firing rate were calculated at both baseline and peak pressure, as previously described [30]. The increase in EUS EMG in response to LPP testing was calculated as the difference in EUS EMG amplitude and frequency between peak pressure during LPP testing and baseline before LPP testing. The mean value of each outcome for each rat was calculated from three or four trials and was used to create a mean and standard error of the mean (SEM) for each experimental group.

Histology

A 5-mm segment of the mid-urethra, attached to the anterior portion of the vagina (5 mm proximal to the urethral meatus), was dissected, immersion fixed in 10% formalin, and

sectioned transversely (5 μm). To identify and quantify the A-PLO-G or A-PLO microbeads retained in the urethral tissue, the samples were examined and numbers of the microbeads were counted in haematoxylin and eosin (H&E)-stained slides. Masson's trichrome-stained slides were analysed quantitatively in a blinded fashion to assess the ratio of collagen to striated and smooth muscle tissue by measuring the area of these two distinct tissues, with collagen stained blue and muscle stained red, in five randomly selected fields per slide at ×200 (Leica Microsystems, Wetzlar, Germany). The analysis was conducted using the colour segmentation tool in the Image Pro Plus analysis software (Media Cybernetics Inc., Silver Spring, MD, USA), which separates features on the acquired image from the background based on their colour characteristics.

Immunohistochemistry—Serial sections were stained for mouse anti-desmin (Dako, Carpinteria, CA, USA), a muscle-specific marker for intermediate filaments in both skeletal and smooth muscle cells; mouse anti-cluster of differentiation 31 (CD31; Thermo Fisher), a marker for endothelial cells; and rabbit anti-neurofilament 200 (Sigma, St. Louis, MO, USA), a marker of innervation. The paraffin-embedded sections were de-paraffinised and subsequently treated for 15 min with citrate buffer (Dako, Palo Alto, CA, USA, pH 6.0), as an antigen retrieval solution, heated to 95 °C. Sections were then stained using a primary antibody diluted with antibody diluents (Dako), followed by a secondary antibody. The sections were exposed to 3,3′-diaminobenzidine (DAB) for 5 min. The sections were then counterstained with haematoxylin for 30 s and cover slipped.

Vessel and Nerve Density—Tissue sections were imaged using an Axiovert 200 inverted microscope (Carl Zeiss Micro-Imaging) with a ×20 objective, and were subsequently analysed using Image-Pro (Media Cybernetics Inc.). Five images per section were quantified for immunocytochemical staining with anti-CD31 and anti-neurofilament antibodies. The number of blood vessels was manually tallied for CD31-stained sections, and used to calculate vessel density using the following formula: Vessel density = number cells expressing CD31 markers/total cells in the tissue area. The number of nerves was manually tallied for neurofilament-stained sections, and used to calculate nerve density using the following formula: Nerve density = number of nerve fibres expressing neurofilament/total cells in the tissue area.

Statistical Analysis

This study was powered to detect a significant difference between the groups in LPP, as the primary outcome. A power analysis indicated that 11 rats/group would provide 80% power to detect an effect size of ≥7 using an ANOVA for a two-sided test with a significance level of $P < 0.05$. Quantitative data are reported as mean ± SEM of data from 11 rats. One-way ANOVA was used for between-group comparison when data was distributed normally, followed by the Student-Neumann–Keuls *post hoc* test for individual group comparisons (SigmaPlot v. 13; Systat Software Inc., San Jose, CA, USA). LPP and EUS EMG data, which were not normally distributed, were analysed using ANOVA on ranks followed by a Tukey *post hoc* test for individual group comparisons (SigmaPlot). In all cases $P < 0.05$ was considered to indicate a statistically significant difference between groups. All measurements were carried out by two investigators blinded to the study group.

Results

Up to 90% of the A-PLO-G microbeads maintained their spherical shape in saline solution at 37 °C for 7 days and after being injected through a 26-G syringe needle. The microbeads were 90–100 μm in diameter (Fig. 1).

IGF-1 Released from A-PLO-G Microbeads *In Vitro*

ELISA data showed that IGF-1 was released at a constant rate from the A-PLO-G microbeads after an initial burst of 40% in the first hour. About 90% of the encapsulated growth factor was released within 36 h, following which the cumulative release increased linearly for 14 days (Fig. 2).

Urethral Function Test

The LPP was significantly lesser in the VD + saline and VD + empty microbead groups compared to the sham group (Fig. 3). In contrast, rats with VD treated with IGF-1 impregnated microbeads (VD + IGF-1 microbeads) had LPP partway between and not significantly different from the sham or VD + saline groups (Fig. 3). The LPP of rats in the VD + IGF-1 microbeads group was however significantly higher than in the VD + empty microbeads group (Fig. 3). Similarly, the increase in amplitude of EUS EMG firing rate with LPP testing was significantly lesser in the VD + saline and VD + empty microbeads groups compared to sham rats (Fig. 3), indicating a reduced guarding reflex. The increase in EUS EMG amplitude in the VD + IGF-1 microbeads group was partway between and not significantly different from that of the other groups. There were no statistically significant differences between the groups in EUS EMG firing rate increase (Fig. 3).

Histology and Immunohistochemistry

H&E staining showed that A-PLO-G microbeads were found around the EUS (Fig. 4) and some were also found in the anterior vaginal wall (<9%). In the VD + saline and VD + empty microbeads groups, disruption and atrophy of striated muscle fibres, as well as collagen infiltration between the EUS muscle fibres were seen compared to the sham group. Muscle fibres were thicker and continuous, and smooth muscle was compact surrounding the urethral epithelium of the sham group (Fig. 5). In addition, the thickness of the EUS was diminished in all VD groups compared to the sham-VD group (Fig. 5). However, treatment with IGF-1 loaded microbeads led to significantly better EUS thickness compared to rats with VD treated with saline or empty microbeads, as well as relatively continuous muscle fibres and near-normal smooth muscle (Fig. 5).

Blood vessel density expressing CD31 was lesser in all VD groups compared to the sham group (Fig. 6), indicating reduced vascularisation with VD. However, treatment with IGF-1 significantly enhanced vessel density compared to the VD + empty microbeads and VD + saline groups. Higher vessel density was associated with enhanced improvement of histological construction and function of EUS muscle tissue (Figs 3,5,6). However, there was no significant difference in innervation and nerve regeneration within the urethral tissue among the IGF-1-A-PLO-G microbeads, IGF-1-empty microbeads and saline injection

groups after VD, as indicated by immunohistochemistry using the neurofilament marker (data not shown).

Discussion

Childbirth injury from vaginal delivery can result in SUI, which damages the EUS, pelvic floor muscles, and neural plexus posterolateral to the vagina [27,31]. SUI occurs in 19% of women aged <45 years, 29% of older women, and 78% of nursing home residents [3]. In addition, a growing number of patients are men [32,33]. SUI affects up to 13 million people in the USA and 200 million worldwide [34], and decreases quality of life, whilst increasing comorbidities such as depression [32,33]. Urine leakage is prevented by the urethra and a supportive apparatus that consists of the anterior vaginal wall and its surrounding muscles and fascial tissues [35]. Whilst the surrounding tissues and pelvic floor musculature are important for maintenance of continence, the urethral musculature is the single most significant contributor to urinary continence in both women and animal models of SUI [36]. Vaginal delivery injures the EUS and muscles of the pelvic floor, as well as disrupting innervation of the EUS [7,37]. Therefore, SUI could be ameliorated if the injured EUS could be restored.

Pelvic floor exercises [10], injection of bulking agents [2–9], and sling surgical procedures [1] are commonly used to treat SUI. Although midurethral slings can reinforce weak pelvic floor muscles and has a 71–73% success rate [1], the urethral sphincter deficiency remains [11]. Over time, bulking agents are absorbed and can cause chronic inflammation, periurethral abscesses, foreign body giant cell responses, erosion into the urinary bladder or the urethra, migration to inner organs, obstruction of the lower urinary tract with resultant urinary retention, severe voiding dysfunction, and even pulmonary embolism [9,12,13].

Injury from vaginal delivery results in symptomatic UI many years after childbirth. The chronic injury sustained by the sphincter muscle and associated nerve structures progresses with time [27,31], suggesting that the deficiencies that occur in the initial childbirth injury do not heal fully. About one-third of women develop SUI postpartum and one-third of those women do not spontaneously recover within 3 months [38]. Those who do recover are at increased risk of developing SUI later in life [39]. Regenerative therapies will undoubtedly work best soon after injury before the muscle has atrophied and prior to the effects of ageing. Therefore, treatment soon after delivery may treat postpartum SUI and prevent later redevelopment of SUI.

No animal undergoes offspring delivery as traumatically as childbirth in humans, even nonhuman primates [40]. Thus, to develop a reliable and predictable animal model of human childbirth, various simulated childbirth injuries have been created [41–43]. The VD model is the most studied and therefore the most validated of the different animal models. In this rat model, the rats develop SUI soon after VD [25] and may redevelop it with oestrus. Thus, the short-term VD model is most applicable to model postpartum SUI, the optimal time to intervene with a regenerative therapy.

Growth factor therapy involves the use of growth factors to promote host tissue healing, by stimulating growth and proliferation of the grafted cells or the resident stem cells involved in tissue healing when used alone or combined with cell-based therapy [44,45]. One advantage of local administration of growth factor therapy is that it could be used in an 'off-the-shelf' fashion to more safely and efficiently stimulate the body's own cells to promote tissue healing [46]. Growth factor therapy may also accelerate the time it takes for tissue injury to repair, resulting in a greater reduction of disability or discomfort. The most commonly used growth factors include: epidermal growth factor (EFG), keratinocyte growth factor (KGF), TGF-α_1 TGF-β_1, TGF-β_2, vascular endothelial growth factor (VEGF), platelet-derived growth factor (PDGF), and IGF-1. Among these growth factors, IGF-1 is the only one that provides multiple functions by promoting muscle regeneration, anti-apoptosis, angiogenesis, and innervation [17].

Microbeads coated with multiple layers of hydrogel are well established and require no viral vectors for growth factor or cell secretion delivery [47]. They have been successfully used to sustain and control release of various drugs targeting specific organs [48]. In addition, several studies have reported the benefits of various hydrogel microbeads for controlled release of growth factors [49], fluorescence protein [50], stem cells [51] or exogenous cells [52], and anti-cancer drugs [53,54] in various experiment models, but not in SUI animal models. Biomaterials based on alginate, PLO and gelatine have been used for a wide variety of biomedical applications due to their biocompatibility and efficacy of drug delivery. However, it is a challenge to control the release of IGF-1 because it has a low molecular weight (7 649 Da) and rapidly releases from regular microbeads such as A-PLO microbeads [21]. The present study is the first to investigate the feasibility of A-PLO-G microbeads loaded with IGF-1 for the treatment of SUI.

A-PLO microbeads are commonly used as a local delivery system for high molecular weight growth factors, such as fibroblast growth factor 2 (FGF2, molecular weight: 22–34 kDa) [55]. The PLO coating can reduce swelling *in vivo* and increase the mechanical strength of alginate microbeads compared to alginate-alone microbeads [21]. Gelatine is a denatured protein obtained by hydrolysis of animal collagen, with either acid or alkaline, and has prominent advantages for biomedical pharmaceutical applications: it is inexpensive, readily available, and has high biocompatibility and biodegradability [56]. Moreover, as a denatured product, gelatine is less antigenic than collagen [57] and contains abundant motifs that can modulate cell adhesion [58]. Due to the different isoelectric points obtained by acid or alkaline processing, the positively or negatively charged gelatine can interact with oppositely charged growth factors to form ionic complexes for a sustained release system [59]. As PLO is a polycationic and gelatine is a polyanionic biomaterial, A-PLO-coated with gelatine can prevent electrostatic interaction of PLO with cells and proteins after implantation [60]. In the present study, we selected to use gelatine as the outer layer of the microbeads to facilitate slow release of IGF-1 and increase retention of the microbeads in the injected site because the hydrophilic properties of gelatine aids the microbeads in binding to the host tissue [60]. Our present data showed that the A-PLO-G microbeads were easily found in the urethral tissue 24 h after injection, whereas no A-PLO microbeads were found.

Insulin-like growth factor 1 released from A-PLO-G microbeads enabled local delivery, exposing the EUS for a prolonged period to IGF-1 with an appropriate dosage gradient. As shown by ELISA, the release kinetics of IGF-1 from A-PLO-G microbeads showed a rapid initial burst, followed by a continuous discharge of the remaining protein for up to 14 days *in vitro.* This release strategy, featuring an initial IGF-1 burst release in the first day, was used as previous work indicated that growth hormones, such as IGF-1, exert their greatest regeneration-promoting effect with anti-inflammatory, vascular development and protection after injury [61].

Whilst the conditions used to evaluate IGF-1 release *in vitro* may not predict the exact protein concentration released *in vivo*, it serves as a useful tool in the design of a drug-delivery system. *In vivo* release of IGF-1 probably occurs over a longer time scale, as tissue surrounding the microbeads provides a diffusive resistance to slow the release of the protein from the microbeads [15]. The advantages of IGF-1-A-PLO-G therefore include: (i) easy processing and controlled release; (ii) excellent stability *in vitro*; (iii) biocompatibility; and (iv) long-term efficiency of IGF-1 release. The size of microbeads, at 100 μm diameter, allows beads to be injected via a small syringe with a 26-G needle. As larger microbeads carry more IGF-1 but a small needle is needed to reduce tissue injury, the size of microbeads used in the present study (90–150 μm diameter) was a compromise between these two important design considerations. For clinical use, a larger needle (18 G, inner diameter 838 μm) could be used in human urethral tissue. Therefore, larger beads (300 μm diameter) with greater IGF-1 carrying capacity could be tested in clinical studies.

As sphincter function plays a critical role in the pathogenesis of SUI, the sphincter muscle injury model is most commonly used to mimic birth trauma [62]. Histologically, VD injury caused significant damage to the EUS in the rat model in the present study, as described previously [63]. Thinner layers of striated muscle fibres and more collagen infiltration were seen 1 week after VD, compared with sham-VD rats. In contrast, the skeletal muscle of the EUS significantly improved after treatment with IGF-1 microbeads and collagen infiltration diminished among the muscle fibres, suggesting the therapeutic effect of IGF-1 is on muscle regeneration. Both the LPP and amplitude of the EUS EMG with LPP testing were not significantly different at 1 week after VD treated with saline only or with empty microbeads, demonstrating that the microbeads themselves do not create a bulking or obstructive effect in the urethra. Similarly, the LPP and amplitude of the EUS EMG with LPP testing significantly improved after VD treated with IGF-1 microbeads compared to saline or empty microbeads treatments, demonstrating initiation of a reparative effect 1 week after VD with IGF-1.

Vascular density was significantly enhanced in the urethra after VD with IGF-1 microbeads compared to saline or empty microbeads, and correlated with enhanced myogenesis in the EUS. This rapid vascularisation in such a short time appears vital to facilitating muscle regeneration, as shown in previous studies in which IGF-1 stimulated myogenesis in regenerating muscle via increasing neovessel formation in injured muscle [64]. Higher vessel density correlated with improved recovery of both structure and function of the EUS muscle, suggesting that increasing angiogenesis promotes muscle regeneration.

Use of IGF-1 resulted in enhanced EUS muscle tissue repair in the early stage of recovery in the present study, but little to no nerve regeneration or innervation was seen in either IGF-1-treated or non-treated groups, compared to the sham control group at 1 week after VD. While IGF-1 is a potent agent for nerve regeneration [65], innervation did not occur within the urethra tissue at 1 week after IGF-1 treatment. The most likely reason is that nerve regeneration requires a longer time. Therefore, one limitation of the present study is the short timeframe after VD that was studied. One week was chosen because LPP returns to normal 10–14 days after VD [25]. However, tissue healing is a complex process that is often divided into three phases with different time courses: bleeding and inflammation (hours), proliferation (days), and remodelling (weeks) [66,67]. Therefore, a longer-term study of EUS tissue repair with IGF-1 treatment is warranted.

Insulin-like growth factor 1 therapy would not be for all pregnant patients after vaginal delivery, but could be implemented for high-risk patients such as women who are overweight or obese, smokers, those with chronic coughing, have a family history of UI, or have had multiple vaginal deliveries. In our opinion, IGF-1 therapy would be better as an early treatment, i.e. postpartum treatment, instead of a delayed treatment, as muscle regeneration is more feasible prior to the muscle atrophy that occurs with age. Women with postpartum UI that does not resolve spontaneously may be a good first target population, as they are at increased risk for SUI development years later. IGF-1 therapy may both treat their postpartum UI and prevent SUI development later. Nonetheless, the optimal time points need further laboratory and clinical investigation.

Conclusions

The present study demonstrated that controlled local release of IGF-1 from IGF-1-A-PLO-G microbeads provides a possible approach for facilitating recovery from SUI induced by childbirth injury, likely mediated via preservation and regeneration of the vasculature. IGF-1-A-PLO-G microbeads represent a promising possible therapy to facilitate recovery from childbirth injuries, treatment of postpartum UI, and possibly prevention of later development of SUI. However, further investigations are needed into long-term effects, degradation of the microbeads, and clinical safety and efficacy.

Acknowledgments

The authors are grateful for R56 DK100669-01A1 support (Principle Investigator: Yuanyuan Zhang), as well as partial support from the Cleveland Clinic and the Rehabilitation R&D Service of the Department of Veterans Affairs (Margot S. Damaser).

Abbreviations:

A-PLO(-G)	alginate-poly-L-ornithine (-gelatine)
CD31	anti-cluster of differentiation 31
EMG	electromyography
EUS	external urethral sphincter

H&E	haematoxylin and eosin
LPP	leak-point pressure
SEM	standard error of the mean
SUI	stress urinary incontinence
VD	vaginal distention

References

1. Wai CY. Surgical treatment for stress and urge urinary incontinence. Obstet Gynecol Clin North Am 2009; 36: 509–19 [PubMed: 19932413]
2. Tsakiris P, de la Rosette JJ, Michel MC, Oelke M. Pharmacologic treatment of male stress urinary incontinence: systematic review of the literature and levels of evidence. Eur Urol 2008; 53: 53–9 [PubMed: 17920183]
3. Moore RD, Serels SR, Davila GW, Settle P. Minimally invasive treatment for female stress urinary incontinence (SUI): a review including TVT, TOT, and mini-sling. Surg Technol Int 2009; 18: 157–73 [PubMed: 19579203]
4. Novara G, Galfano A, Boscolo-Berto R et al. Complication rates of tension-free midurethral slings in the treatment of female stress urinary incontinence: a systematic review and meta-analysis of randomized controlled trials comparing tension-free midurethral tapes to other surgical procedures and different devices. Eur Urol 2008; 53: 288–308 [PubMed: 18031923]
5. Novara G, Ficarra V, Boscolo-Berto R, Secco S, Cavalleri S, Artibani W. Tension-free midurethral slings in the treatment of female stress urinary incontinence: a systematic review and meta-analysis of randomized controlled trials of effectiveness. Eur Urol 2007; 52: 663–78 [PubMed: 17601652]
6. Neumann PB, Grimmer KA, Deenadayalan Y. Pelvic floor muscle training and adjunctive therapies for the treatment of stress urinary incontinence in women: a systematic review. BMC Womens Health 2006; 6: 11 [PubMed: 16805910]
7. Mariappan P, Alhasso A, Ballantyne Z, Grant A, N'Dow J. Duloxetine, a serotonin and noradrenaline reuptake inhibitor (SNRI) for the treatment of stress urinary incontinence: a systematic review. Eur Urol 2007; 51: 67–74 [PubMed: 17014950]
8. Trost L, Elliott DS. Male stress urinary incontinence: a review of surgical treatment options and outcomes. Adv Urol 2012; 2012: 287489 [PubMed: 22649446]
9. Kotb AF, Campeau L, Corcos J. Urethral bulking agents: techniques and outcomes. Curr Urol Rep 2009; 10: 396–400 [PubMed: 19709488]
10. Caruso DJ, Gomez CS, Gousse AE. Medical management of stress urinary incontinence: is there a future? Curr Urol Rep 2009; 10: 401–7 [PubMed: 19709489]
11. Novara G, Artibani W. Myoblasts and fibroblasts in stress urinary incontinence. Lancet 2007; 369: 2139–40 [PubMed: 17604781]
12. Kiilholma PJ, Chancellor MB, Makinen J, Hirsch IH, Klemi PJ. Complications of Teflon injection for stress urinary incontinence. Neurourol Urodyn 1993; 12: 131–7 [PubMed: 7920669]
13. Koski ME, Enemchukwu EA, Padmanabhan P, Kaufman MR, Scarpero HM, Dmochowski RR. Safety and efficacy of sling for persistent stress urinary incontinence after bulking injection. Urology 2011; 77: 1076–80 [PubMed: 21216448]
14. Nakamichi M, Akishima-Fukasawa Y, Fujisawa C, Mikami T, Onishi K, Akasaka Y. Basic fibroblast growth factor induces angiogenic properties of fibrocytes to stimulate vascular formation during wound healing. Am J Pathol 2016; 186: 3203–16 [PubMed: 27773739]
15. Liu G, Pareta RA, Wu R et al. Skeletal myogenic differentiation of urine-derived stem cells and angiogenesis using microbeads loaded with growth factors. Biomaterials 2013; 34: 1311–26 [PubMed: 23137393]
16. Amsden B Novel biodegradable polymers for local growth factor delivery. Eur J Pharm Biopharm 2015; 97: 318–28 [PubMed: 26614555]

17. Musarò A, McCullagh K, Paul A et al. Localized IGF-1 transgene expression sustains hypertrophy and regeneration in senescent skeletal muscle. Nat Genet 2001; 27: 195–200 [PubMed: 11175789]
18. Rosenbloom AL. The role of recombinant insulin-like growth factor I in the treatment of the short child. Curr Opin Pediatr 2007; 19: 458–64 [PubMed: 17630612]
19. Wei W, Howard PS, Macarak EJ. Recombinant insulin-like growth factor-1 activates satellite cells in the mouse urethral rhabdosphincter. BMC Urol 2013; 13: 62 [PubMed: 24279352]
20. Cittadini A, Monti MG, Petrillo V et al. Complementary therapeutic effects of dual delivery of insulin-like growth factor-1 and vascular endothelial growth factor by gelatin microspheres in experimental heart failure. Eur J Heart Fail 2011; 13: 1264–74 [PubMed: 22045926]
21. Darrabie MD, Kendall WF Jr, Opara EC. Characteristics of poly-L-ornithine-coated alginate microcapsules. Biomaterials 2005; 26: 6846–52 [PubMed: 15955558]
22. Pan HQ, Kerns JM, Lin DL, Liu S, Esparza N, Damaser MS. Increased duration of simulated childbirth injuries results in increased time to recovery. Am J Physiol Regul Integr Comp Physiol 2007; 292: R1738–44 [PubMed: 17204590]
23. Hakim L, Endo M, Feola A et al. High-frequency micro-ultrasound: a novel method to assess external urethral sphincter function in rats following simulated birth injury. Neurourol Urodyn 2015; 34: 264–9 [PubMed: 24436081]
24. Dissaranan C, Cruz MA, Kiedrowski MJ et al. Rat mesenchymal stem cell secretome promotes elastogenesis and facilitates recovery from simulated childbirth injury. Cell Transplant 2014; 23: 1395–406 [PubMed: 23866688]
25. Jiang HH, Pan HQ, Gustilo-Ashby MA et al. Dual simulated childbirth injuries result in slowed recovery of pudendal nerve and urethral function. Neurourol Urodyn 2009; 28: 229–35 [PubMed: 18973146]
26. Cannon TW, Wojcik EM, Ferguson CL, Saraga S, Thomas C, Damaser MS. Effects of vaginal distension on urethral anatomy and function. BJU Int 2002; 90: 403–7 [PubMed: 12175397]
27. Phull HS, Pan HQ, Butler RS, Hansel DE, Damaser MS. Vulnerability of continence structures to injury by simulated childbirth. Am J Physiol Renal Physiol 2011; 301: F641–9 [PubMed: 21613415]
28. Cannon TW, Damaser MS. Effects of anesthesia on cystometry and leak point pressure of the female rat. Life Sci 2001; 69: 1193–202 [PubMed: 11508351]
29. Pan HQ, Kerns JM, Lin DL et al. Dual simulated childbirth injury delays anatomic recovery. Am J Physiol Renal Physiol 2009; 296: F277–83 [PubMed: 19091786]
30. Steward JE, Clemons JD, Zaszczurynski PJ, Butler RS, Damaser MS, Jiang HH. Quantitative evaluation of electrodes for external urethral sphincter electromyography during bladder-to-urethral guarding reflex. World J Urol 2010; 28: 365–71 [PubMed: 19680661]
31. Li TS, Cheng K, Malliaras K et al. Expansion of human cardiac stem cells in physiological oxygen improves cell production efficiency and potency for myocardial repair. Cardiovasc Res 2011; 89: 157–65 [PubMed: 20675298]
32. Sampselle CM, Miller JM, Mims BL, Delancey JO, Ashton-Miller JA, Antonakos CL. Effect of pelvic muscle exercise on transient incontinence during pregnancy and after birth. Obstet Gynecol 1998; 91: 406–12 [PubMed: 9491869]
33. Markland AD, Goode PS, Redden DT, Borrud LG, Burgio KL. Prevalence of urinary incontinence in men: results from the national health and nutrition examination survey. J Urol 2010; 184: 1022–7 [PubMed: 20643440]
34. Wilson L, Brown JS, Shin GP, Luc KO, Subak LL. Annual direct cost of urinary incontinence. Obstet Gynecol 2001; 98: 398–406 [PubMed: 11530119]
35. Delancey JO. Why do women have stress urinary incontinence? Neurourol Urodyn 2010; 29 (Suppl. 1): S13–7 [PubMed: 20419794]
36. Morgan DM, Umek W, Guire K, Morgan HK, Garabrant A, DeLancey JO. Urethral sphincter morphology and function with and without stress incontinence. J Urol 2009; 182: 203–9 [PubMed: 19450822]
37. Sajadi KP, Gill BC, Damaser MS. Neurogenic aspects of stress urinary incontinence. Curr Opin Obstet Gynecol 2010; 22: 425–9 [PubMed: 20706117]

38. Mason L, Glenn S, Walton I, Appleton C. The prevalence of stress incontinence during pregnancy and following delivery. Midwifery 1999; 15: 120–8 [PubMed: 10703415]
39. Viktrup L, Lose G, Rolff M, Barfoed K. The symptom of stress incontinence caused by pregnancy or delivery in primiparas. Obstet Gynecol 1992; 79: 945–9 [PubMed: 1579319]
40. Trevathan WR. The evolution of bipedalism and assisted birth. Med Anthropol Q 1996; 10: 287–90 [PubMed: 8744088]
41. Jiang HH, Damaser MS. Animal models of stress urinary incontinence. Handb Exp Pharmacol 2011; 202: 45–67
42. Gill BC, Moore C, Damaser MS. Postpartum stress urinary incontinence: lessons from animal models. Expert Rev Obstet Gynecol 2010; 5: 567–80 [PubMed: 21113428]
43. Hijaz A, Daneshgari F, Sievert KD, Damaser MS. Animal models of female stress urinary incontinence. J Urol 2008; 179: 2103–10 [PubMed: 18423691]
44. Hardwicke J, Schmaljohann D, Boyce D, Thomas D. Epidermal growth factor therapy and wound healing–past, present and future perspectives. Surgeon 2008; 6: 172–7 [PubMed: 18581754]
45. Kalay Z, Cevher SC. Oxidant and antioxidant events during epidermal growth factor therapy to cutaneous wound healing in rats. Int Wound J 2012; 9: 362–71 [PubMed: 22129466]
46. Sumino Y, Yoshikawa S, Mimata H, Yoshimura N. Therapeutic effects of IGF-1 on stress urinary incontinence in rats with simulated childbirth trauma. J Urol 2014; 191: 529–38 [PubMed: 24036237]
47. McQuilling JP, Arenas-Herrera J, Childers C et al. New alginate microcapsule system for angiogenic protein delivery and immunoisolation of islets for transplantation in the rat omentum pouch. Transplant Proc 2011; 43: 3262–4 [PubMed: 22099771]
48. Nakase H, Okazaki K, Tabata Y et al. New cytokine delivery system using gelatin microspheres containing interleukin-10 for experimental inflammatory bowel disease. J Pharmacol Exp Ther 2002; 301: 59–65 [PubMed: 11907157]
49. Impellitteri NA, Toepke MW, Lan Levengood SK, Murphy WL. Specific VEGF sequestering and release using peptide-functionalized hydrogel microspheres. Biomaterials 2012; 33: 3475–84 [PubMed: 22322198]
50. Shibata H, Heo YJ, Okitsu T, Matsunaga Y, Kawanishi T, Takeuchi S. Injectable hydrogel microbeads for fluorescence-based in vivo continuous glucose monitoring. Proc Natl Acad Sci USA 2010; 107: 17894–8 [PubMed: 20921374]
51. Zhou H, Xu HH. The fast release of stem cells from alginate-fibrin microbeads in injectable scaffolds for bone tissue engineering. Biomaterials 2011; 32: 7503–13 [PubMed: 21757229]
52. Li W, Lee S, Ma M et al. Microbead-based biomimetic synthetic neighbors enhance survival and function of rat pancreatic beta-cells. Sci Rep 2013; 3: 2863 [PubMed: 24091640]
53. Li S, Chen N, Gaddes ER, Zhang X, Dong C, Wang Y. A Droserabioinspired hydrogel for catching and killing cancer cells. Sci Rep 2015; 5: 14297 [PubMed: 26396063]
54. Li M, Tang Z, Zhang D et al. Doxorubicin-loaded polysaccharide nanoparticles suppress the growth of murine colorectal carcinoma and inhibit the metastasis of murine mammary carcinoma in rodent models. Biomaterials 2015; 51: 161–72 [PubMed: 25771007]
55. Chlebova K, Bryja V, Dvorak P, Kozubik A, Wilcox WR, Krejci P. High molecular weight FGF2: the biology of a nuclear growth factor. Cell Mol Life Sci 2009; 66: 225–35 [PubMed: 18850066]
56. Iwamoto S, Nakagawa K, Sugiura S, Nakajima M. Preparation of gelatin microbeads with a narrow size distribution using microchannel emulsification. AAPS PharmSciTech 2002; 3: E25 [PubMed: 12916940]
57. Elzoghby AO, Samy WM, Elgindy NA. Protein-based nanocarriers as promising drug and gene delivery systems. J Control Release 2012; 161: 38–49 [PubMed: 22564368]
58. Wang H, Boerman OC, Sariibrahimoglu K, Li Y, Jansen JA, Leeuwenburgh SC. Comparison of micro- vs. nanostructured colloidal gelatin gels for sustained delivery of osteogenic proteins: bone morphogenetic protein-2 and alkaline phosphatase. Biomaterials 2012; 33: 8695–703 [PubMed: 22922022]
59. Zhu XH, Tabata Y, Wang CH, Tong YW. Delivery of basic fibroblast growth factor from gelatin microsphere scaffold for the growth of human umbilical vein endothelial cells. Tissue Eng Part A 2008; 14: 1939–47 [PubMed: 18636948]

60. Pinkas O, Goder D, Noyvirt R, Peleg S, Kahlon M, Zilberman M. Structuring of composite hydrogel bioadhesives and its effect on properties and bonding mechanism. Acta Biomater 2017; 51: 125–37 [PubMed: 28110072]

61. Puche JE, Castilla-Cortazar I. Human conditions of insulin-like growth factor-I (IGF-I) deficiency. J Transl Med 2012; 10: 224 [PubMed: 23148873]

62. Lin CS, Lue TF. Stem cell therapy for stress urinary incontinence: a critical review. Stem Cells Dev 2012; 21: 834–43 [PubMed: 22121849]

63. Damaser MS, Broxton-King C, Ferguson C, Kim FJ, Kerns JM. Functional and neuroanatomical effects of vaginal distention and pudendal nerve crush in the female rat. J Urol 2003; 170: 1027–31 [PubMed: 12913764]

64. Rabinovsky ED, Draghia-Akli R. Insulin-like growth factor I plasmid therapy promotes in vivo angiogenesis. Mol Ther 2004; 9: 46–55 [PubMed: 14741777]

65. Apel PJ, Ma J, Callahan M et al. Effect of locally delivered IGF-1 on nerve regeneration during aging: an experimental study in rats. Muscle Nerve 2010; 41: 335–41 [PubMed: 19802878]

66. Prisk V, Huard J. Muscle injuries and repair: the role of prostaglandins and inflammation. Histol Histopathol 2003; 18: 1243–56 [PubMed: 12973691]

67. Tidball JG. Inflammatory processes in muscle injury and repair. Am J Physiol Regul Integr Comp Physiol 2005; 288: R345–53 [PubMed: 15637171]

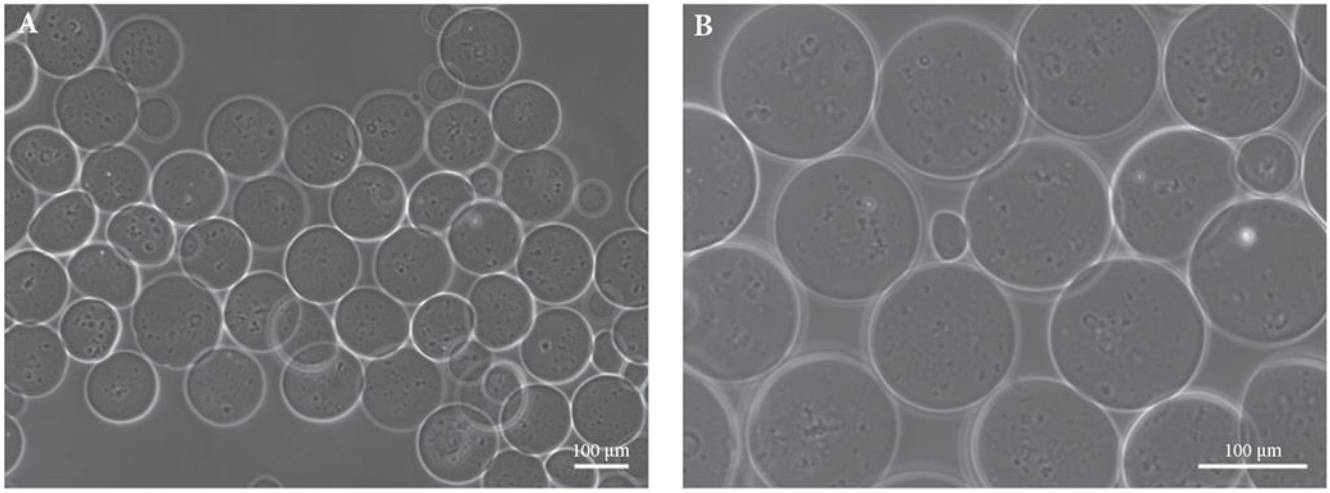

Fig. 1.

Morphology of microbeads in saline solution at 37 °C (**A**) at 1 h and (**B**) 7 days after fabrication. The microbeads maintained consistency in size and integrity in shape in saline solution after injection into a culture dish via a 26-G syringe. Scale bar: 100 μm.

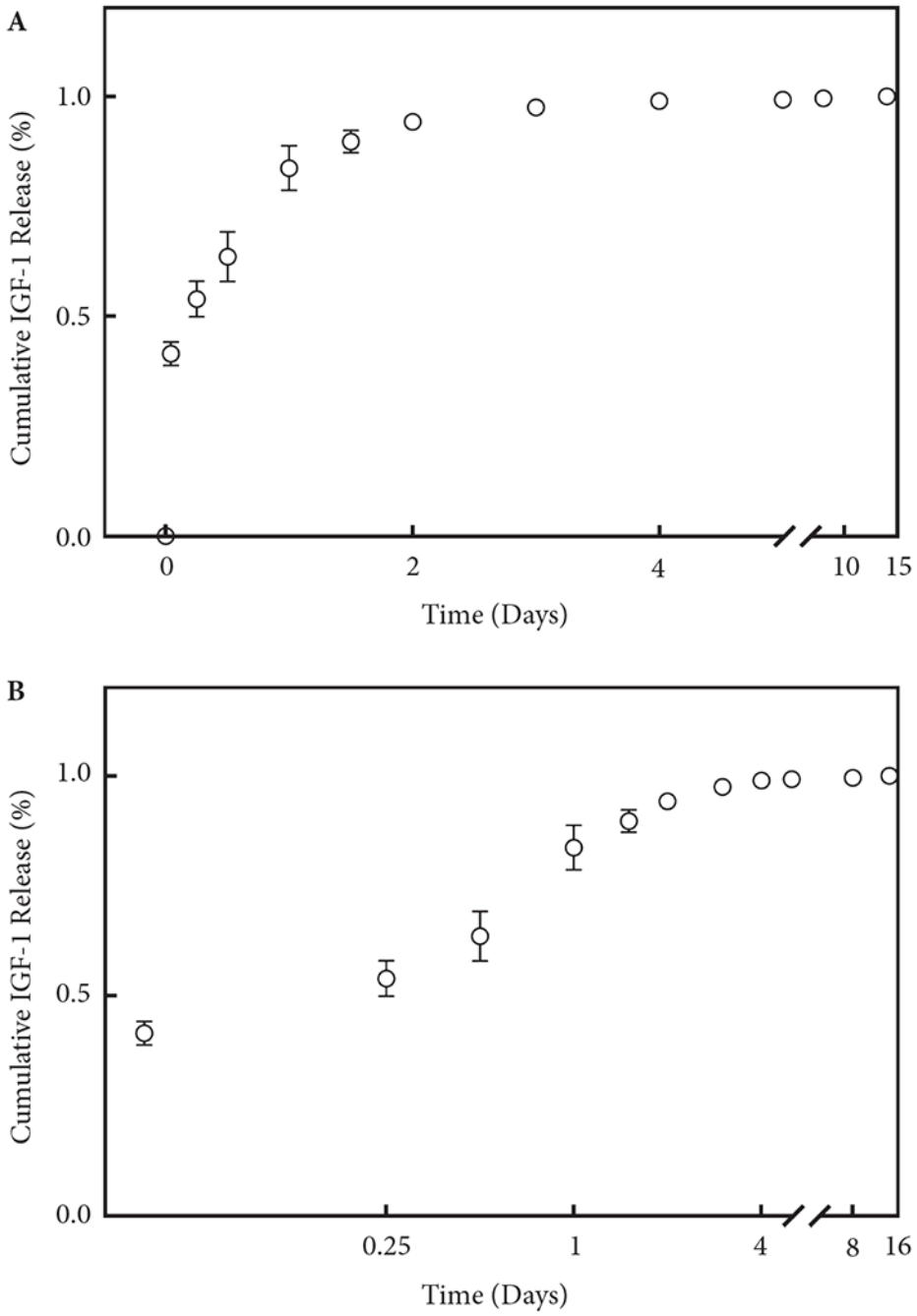

Fig. 2.

Cumulative IGF-1 release profile and activity from A-PLO-G microbeads by (**A**) ELISA in both linear and (**B**) log scales. Each symbol represents mean ± SEM of 11 samples. The curve is plotted by the release percentage with standard deviation, based on three different tests.

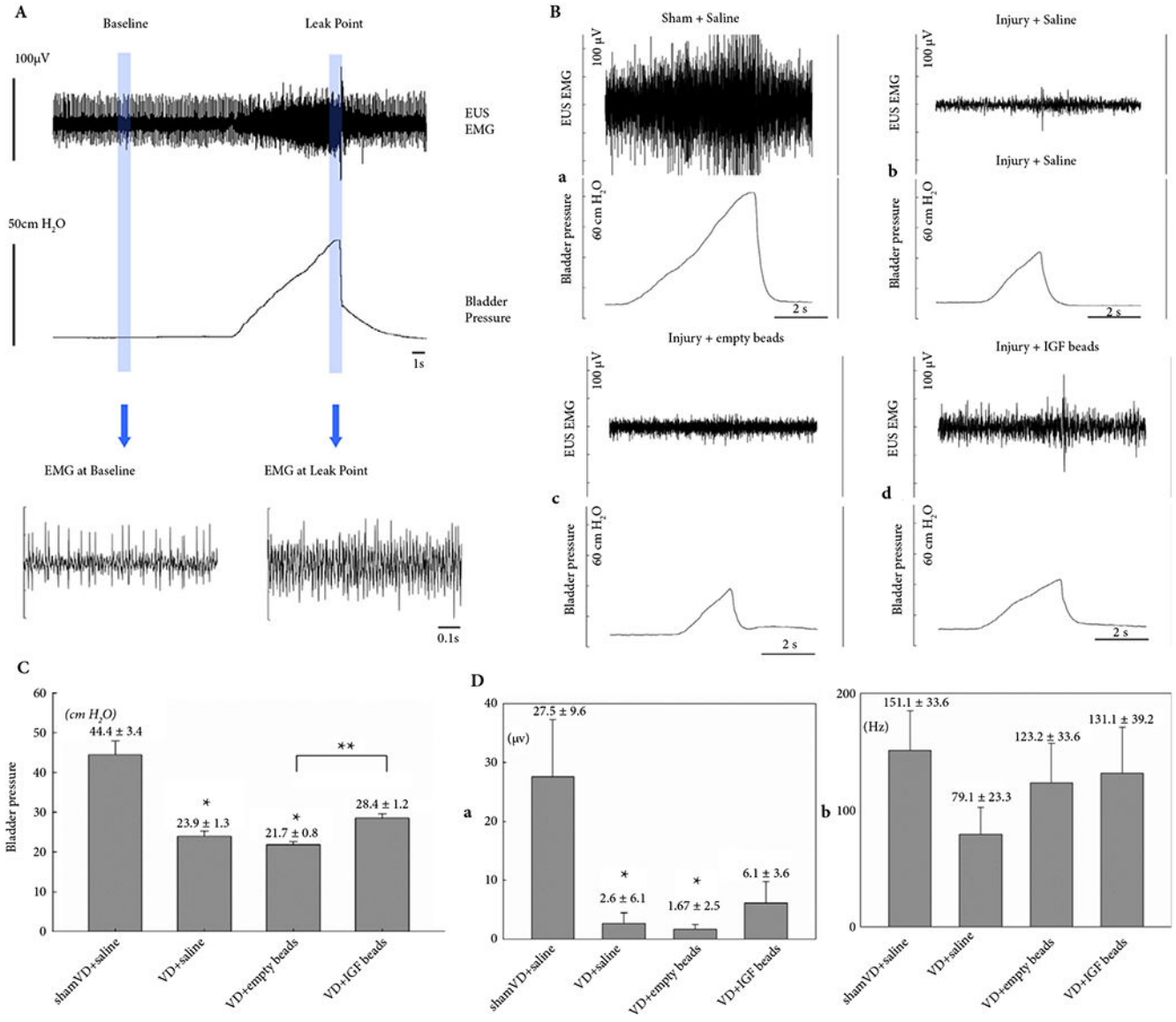

Fig. 3.

(**A**) Representative examples of LPP and EUS EMG data from a sham-VD rat. The slow rise to peak in bladder pressure is from external pressure applied to the bladder. When leakage occurs, the external pressure is rapidly removed and the pressure quickly drops back to baseline. The vertical lines indicate the 1-s segments used for quantitative data analysis. (**B**) Representative examples of EUS EMG and LPP results at 1 week after (**a**) sham-VD treated with saline, (**b**) VD treated with saline, (**c**) VD treated with empty microbeads, and (**d**) VD treated with IGF-1 loaded microbeads. (**C**) LPP results. Each bar represents mean ± SEM of data from 11 rats. *Indicates a significant difference compared with the sham-VD + saline group with $P < 0.05$. **Indicates a significant difference compared with the VD + empty beads group with $P < 0.05$. (**D**) EUS EMG results. (**a**) Amplitude increase and (**b**) firing rate increase are shown as mean ± SEM of data from 11 rats. *Indicates a significant difference compared with the sham-VD + saline group with $P < 0.05$.

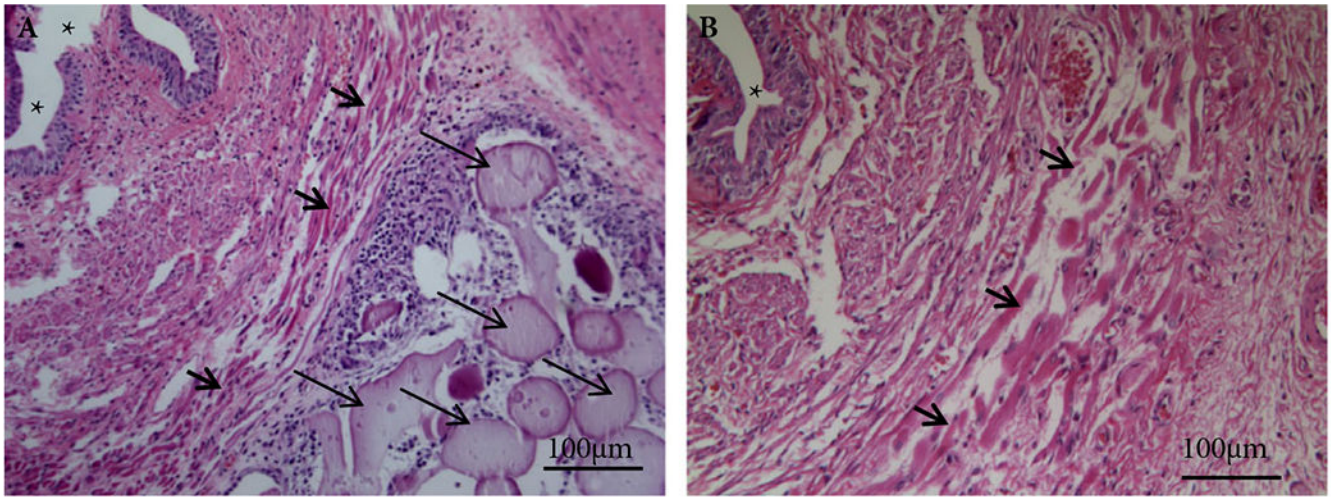

Fig. 4.

Histological cross-sections of urethral tissue after injection of microbeads. H&E staining and Masson's trichrome staining showed that: (**A**) A-PLO-G microbeads (long thin arrowheads) were seen around the EUS (short thick arrowheads) 7 days after implantation, (**B**) but no A-PLO microbeads appeared. Note: *indicating the urethral lumen. Scale bar: 100 μm ×200.

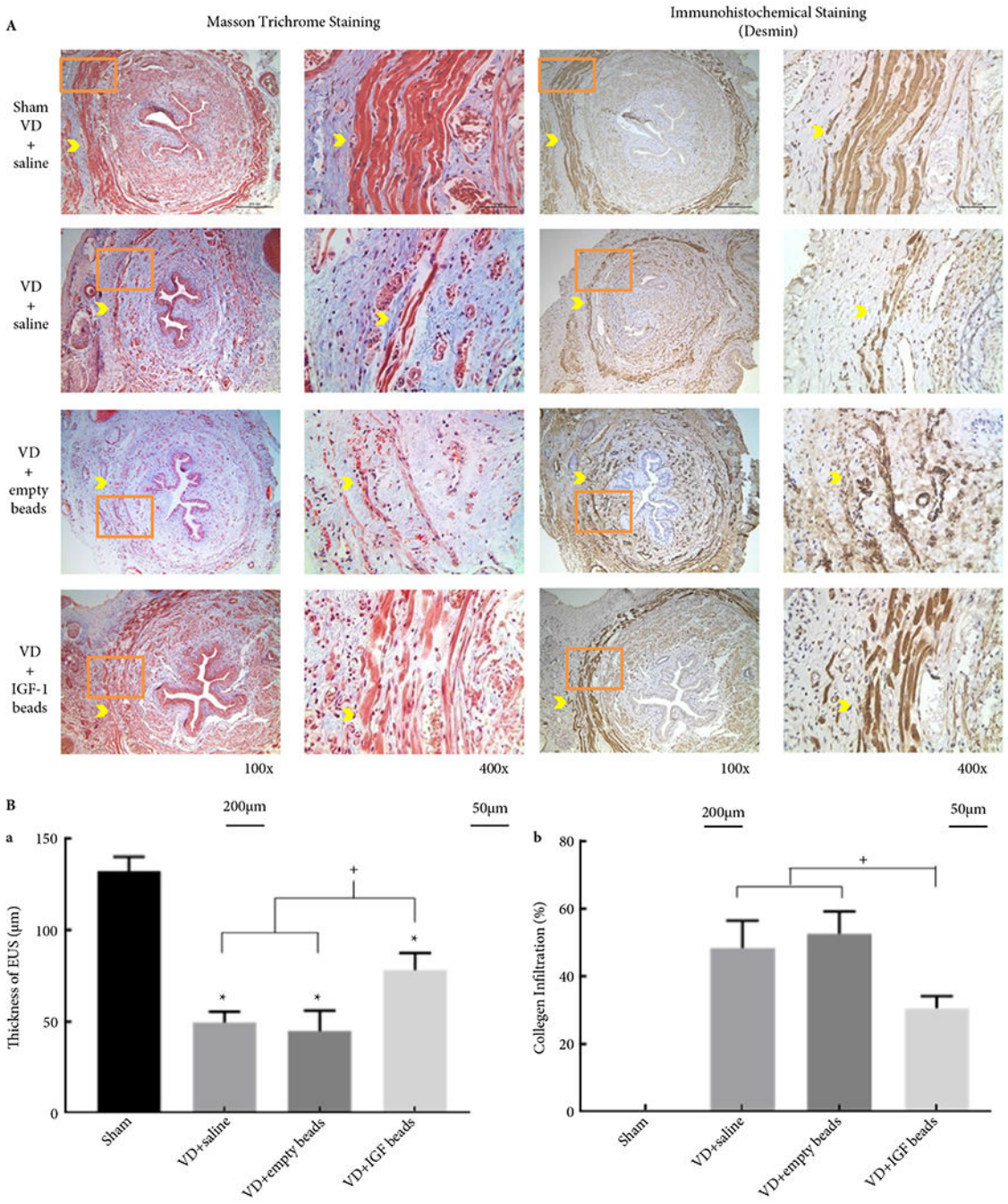

Fig. 5.

(**A**) Example Masson's trichrome-stained and immunofluorescent-stained (desmin) transverse sections of urethras from rats in all experimental groups. The orange box in the left panel indicates the location of the corresponding higher magnification picture in the right panel. Bars = 200 μm in left panel and bars = 50 μm in the right panel. Yellow arrowhead indicates urethral striated muscle within EUS. (**B**) Thickness of striated muscle within EUS (**a**) and collagen infiltration (**b**). *Indicates a significant reduction of thickness of EUS in all VD groups, + shows that the IGF-1 bead-treated group improved thickness of

the EUS and reduced collagen infiltration compared to the saline-or empty beads-treated groups ($P < 0.05$).

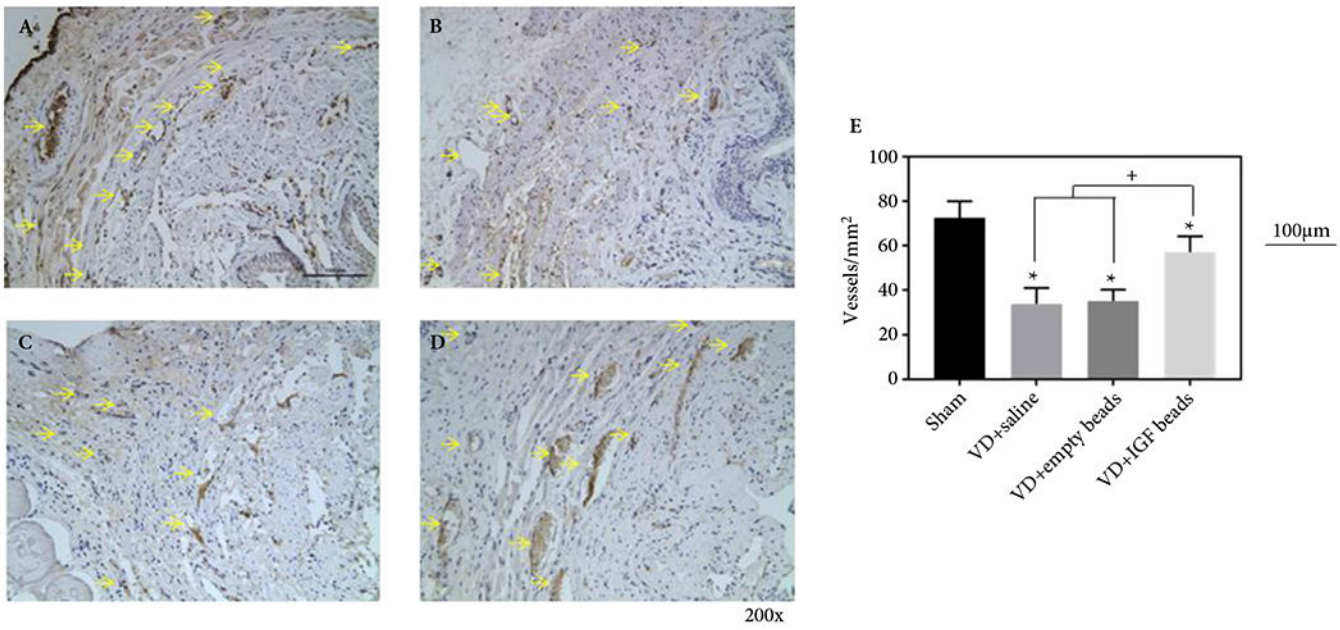

Fig. 6.

Representative examples of CD31 immunohistochemical stained transverse sections of urethras from sham rats treated with saline (**A**), VD rats treated with saline (**B**), VD rats treated with empty microbeads (**C**), and VD rats treated with IGF-1 loaded A-PLO-G microbeads (**D**). The scale bar equals 100 μm in (**A**). Density of CD31 positive structures (**E**) determined from immunohistochemical stains. *Indicates the significant reduction of density of vessel in all VD groups. + shows that there was a higher density of CD31-stained vessels in rats treated with IGF-1 beads compared to those treated with empty beads or saline ($P < 0.05$).